Corrections

CHEMISTRY, BIOCHEMISTRY. For the article "6-Ethynylthieno[3,2-d]- and 6-ethynylthieno[2,3-d]pyrimidin-4-anilines as tunable covalent modifiers of ErbB kinases," by Edgar R. Wood, Lisa M. Shewchuk, Byron Ellis, Perry Brignola, Ronald L. Brashear, Thomas R. Caferro, Scott H. Dickerson, Hamilton D. Dickson, Kelly H. Donaldson, Michael Gaul, Robert J. Griffin, Anne M. Hassell, Barry Keith, Robert Mullin, Kimberly G. Petrov, Michael J. Reno,

David W. Rusnak, Sarva M. Tadepalli, John C. Ulrich, Craig D. Wagner, Dana E. Vanderwall, Alex G. Waterson, Jon D. Williams, Wendy L. White, and David E. Uehling, which appeared in issue 8, February 26, 2008, of *Proc Natl Acad Sci USA* (105:2773–2778; first published February 19, 2008; 10.1073/pnas.0708281105), the authors note that, in Fig. 3*B*, a green block obscures the ligand. The corrected figure and its legend appear below.
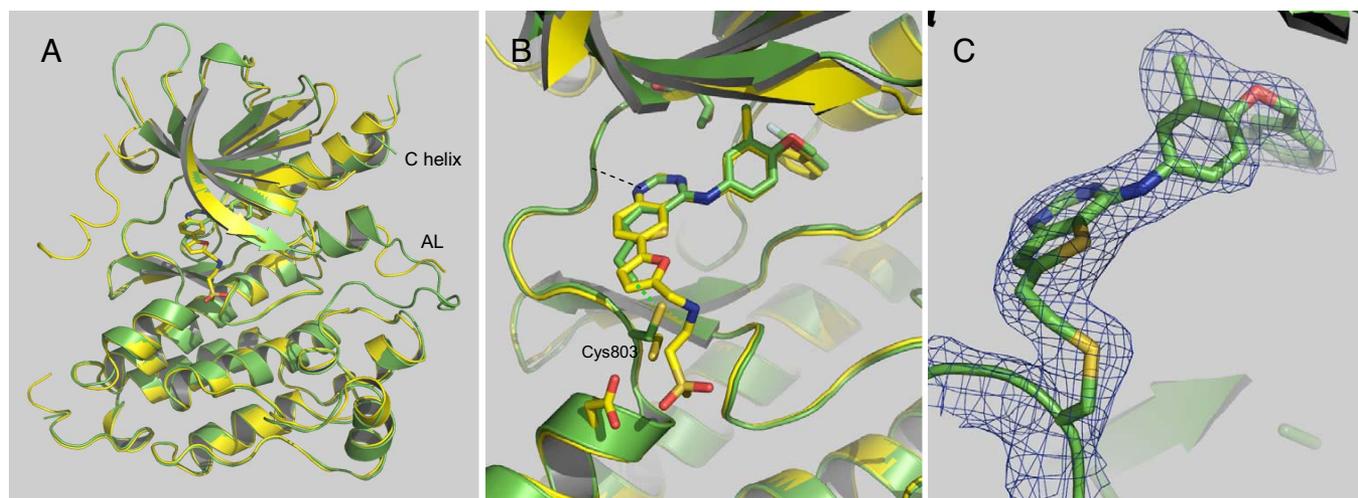

Fig. 3. X-ray crystal structure of thienopyrimidine **6** in ErbB-4. (*A*) Overlay of the ErbB-4 complexed with **6** (green) and EGFR complexed with lapatinib (yellow). (*B*) Overlay of the active sites of ErbB-4 (green) and EGFR (yellow). The covalent bond between ErbB-4 and **6** is shown as a dotted green line. The location of a hydrogen bond between the pyrimidine N1 of **6** and the hinge region of ErbB-4 is shown by a dashed line. (*C*) Omit map density for the ErbB-4 inhibitor complex contoured at 1 sigma.

BIOPHYSICS. For the article "Charge transport and intrinsic fluorescence in amyloid-like fibrils," by Loretta Laureana del Mercato, Pier Paolo Pompa, Giuseppe Maruccio, Antonio Della Torre, Stefania Sabella, Antonio Mario Tamburro, Roberto Cingolani, and Ross Rinaldi, which appeared in issue 46, November 13, 2007, of *Proc Natl Acad Sci USA* (104:18019–18024; first published November 5, 2007; 10.1073/pnas.0702843104), the authors wish to add a reference to a paper by A. Shukla *et al.* (35), in which an intrinsic, nonaromatic fluorescence emission with the same excitation and emission characteristics was observed in different protein crystals and aggregates, upon UV-A excitation, and was attributed to the delocalization of peptide electrons by intra- and/or intermolecular hydrogen bond formation, consistent with the intrinsic blue–green fluorescence we report in amyloid-like nanofibrils. The added reference appears below.

35. Shukla A, Mukherjee S, Sharma S, Agrawal V, Radha Kishan KV, Guptasarma P (2004) *Arch Biochem Biophys* 428:144–153.

6-Ethynylthieno[3,2-d]- and 6-ethynylthieno[2,3-d]pyrimidin-4-anilines as tunable covalent modifiers of ErbB kinases

Edgar R. Wood[a], Lisa M. Shewchuk[b], Byron Ellis[c], Perry Brignola[c], Ronald L. Brashear[d], Thomas R. Caferro[e], Scott H. Dickerson[b], Hamilton D. Dickson[e], Kelly H. Donaldson[e], Michael Gaul[e], Robert J. Griffin[f], Anne M. Hassell[b], Barry Keith[g], Robert Mullin[g], Kimberly G. Petrov[e], Michael J. Reno[e], David W. Rusnak[g], Sarva M. Tadepalli[f], John C. Ulrich[f], Craig D. Wagner[a], Dana E. Vanderwall[b], Alex G. Waterson[e], Jon D. Williams[b], Wendy L. White[b], and David E. Uehling[e,h]

Departments of [a]Assay Development, [b]Computational and Structural Sciences, [c]Biological Reagents and Assay Development, [f]Metabolic DMPK, [e]Oncology Chemistry, [d]Physical Properties and Developability, and [g]Oncology Biology, GlaxoSmithKline, Research Triangle Park, NC 27709

Analysis of the x-ray crystal structure of mono-substituted acetylenic thienopyrimidine 6 complexed with the ErbB family enzyme ErbB-4 revealed a covalent bond between the terminal carbon of the acetylene moiety and the sulfhydryl group of Cys-803 at the solvent interface. The identification of this covalent adduct suggested that acetylenic thienopyrimidine 6 and related analogs might also be capable of forming an analogous covalent adduct with EGFR, which has a conserved cysteine (797) near the ATP binding pocket. To test this hypothesis, we treated a truncated, catalytically competent form of EGFR (678–1020) with a structurally related propargylic amine (8). An investigation of the resulting complex by mass spectrometry revealed the formation of a covalent complex of thienopyrimidine 8 with Cys-797 of EGFR. This finding enabled us to readily assess the irreversibility of various inhibitors and also facilitated a structure–activity relationship understanding of the covalent modifying potential and biological activity of a series of acetylenic thienopyrimidine compounds with potent antitumor activity. Several ErbB family enzyme and cell potent 6-ethynyl thienopyrimidine kinase inhibitors were found to form covalent adducts with EGFR.

inhibitors | enzyme | irreversible | thiol | alkylation

Inhibition of the ErbB family receptor tyrosine kinases (EGFR, ErbB-2) represents a major advance in the treatment of solid tumors, as demonstrated by the promising clinical activity of gefitinib (1), erlotinib (2), and lapatinib (3) (Fig. 1) (1). These drugs are selective, reversible ATP-competitive EGFR (e.g., 1, 2) or dual EGFR/ErbB-2 inhibitors (3), respectively. An alternative approach for targeting this family of enzymes has been through irreversible alkylation of an ErbB family-conserved cysteine residue (Cys-797 in EGFR, Cys-805 in ErbB-2, and Cys-803 in ErbB-4).[i] This latter approach led to the discovery of the potent, irreversible agents canertinib (4) and pelitinib (5) (Fig. 1) (2, 3). Both compounds 4 and 5 and other irreversible agents are reported to be in phase II clinical trials (4).

To identify potent, efficacious EGFR/ErbB-2 inhibitors structurally distinct from lapatinib, a series of 4-anilino thienopyrimidines containing the fluorobenzyl aniline subunit common to 3 was explored. Optimization of this series on enzyme and cellular assays led to the identification of 6-ethynyl-substituted thieno[3,2-d]pyrimidines and thieno[2,3-d]pyrimidines as represented by the general structures **A** and **B,** respectively (Fig. 2) (5–7). Several of these analogs were found to be potent inhibitors of purified EGFR and ErbB-2 and the proliferation of tumor cells that highly express these kinases.

To evaluate their binding mode in the ErbB family enzyme active site, representative inhibitors in this series were cocrystallized with an ErbB-4 construct (690–999) that has high homology to EGFR

and ErbB2 and whose preparation and stability is suitable for x-ray crystallographic studies. Success in this effort was initially achieved by using the ethynyl derivative **6**, which after cocrystallization with ErbB-4 led to the formation of crystals suitable for further analysis. Surprisingly, although **6** and its congeners do not possess an obvious electrophilic Michael acceptor such as the α,β-unsaturated amides in quinazolines **4** and **5**, x-ray analysis of the structure revealed the existence of a covalent bond between the terminal acetylenic carbon and the sulfhydryl of Cys-803 in ErbB-4 (Fig. 3). This finding led us to suspect that formation of covalent adducts with ErbB family enzymes might be a general phenomenon within this series.

To further probe this possibility, a method to detect the covalent modification of the EGFR construct by electrospray mass spectrometry (MS) was developed. In this method, a 1 μM solution of a truncated, catalytically competent form of EGFR (678–1020) was subjected to an excess of the drug candidate and the molecular mass of the protein was then evaluated by using liquid chromatography-mass spectrometry (LC/MS). By using the irreversible ErbB kinase inhibitor canertinib (**4**) as a prototype, the rapid (<10 min), complete formation of a protein complex with a molecular mass 485 mass units greater than the EGFR construct was detected, which is indicative of a covalent adduct of the protein plus **4**. In contrast, treatment of the protein with **3** (lapatinib) failed to impact the observed molecular mass of the protein. These observations therefore demonstrated this LC/MS method was capable of distinguishing between a covalent inhibitor of EGFR and a noncovalent, irreversible inhibitor. With this facile tool for studying alkylation, the propensity of analogs in series A and B to form covalent adducts was evaluated, and their alkylation ability was compared with other biological properties of these analogs.

© 2008 by The National Academy of Sciences of the USA
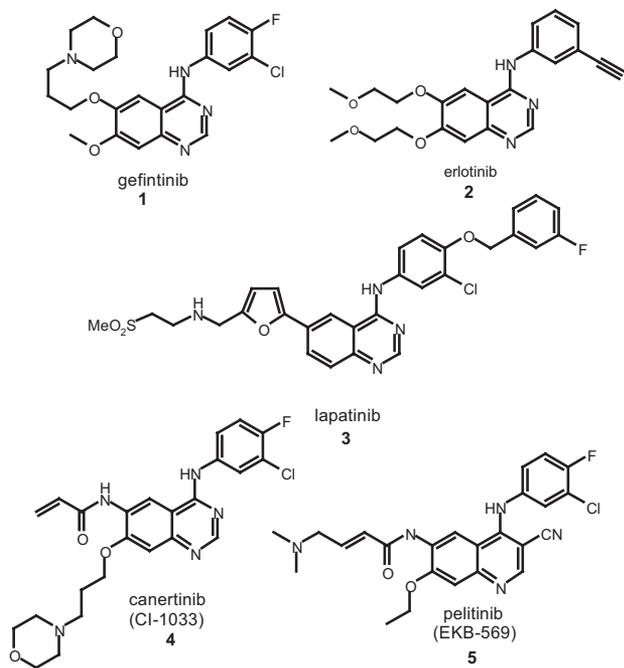
Fig. 1. EGFR and ErbB-2 kinase inhibitors under clinical investigation.

[3,2-d] Thienopyrimidines   [2,3-d] Thienopyrimidines

Fig. 2. 6-Ethynylthieno[3,2-d]- and 6-Ethynylthieno[2,3-d]pyrimidin-4-anilines A and B.

Results

Enzyme and Cellular Inhibition Studies. A series of 6-ethynylthieno[3,2-d]pyrimidin-4-anilines and 6-ethynylthieno[2,3-d]pyrimidin-4-anilines were tested for inhibition of EGFR (671–1210)-, ErbB-2 (691–1255)-, and ErbB-4 (690–1309)-mediated phosphorylation of peptide substrate (8). Because some of these analogs have the ability to alkylate the enzyme and are therefore time-dependent inhibitors, the IC_{50} values can change as a function of time. Therefore, the IC_{50} values presented are relative based on the incubation time of the enzyme assay (40 min for the three constructs) and should not be used to draw conclusions about absolute potency.

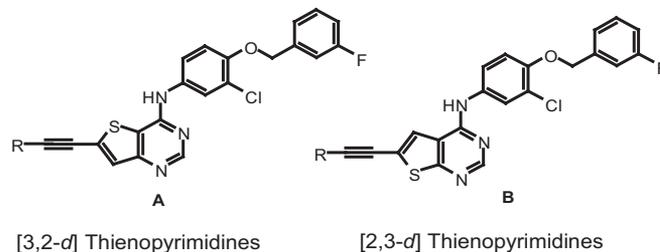In addition to evaluating enzyme inhibition, these analogs were tested for their ability to inhibit proliferation of EGFR-overexpressing (HN5) and ErbB-2-overexpressing (BT474) cell lines and normal human foreskin fibroblast (HFF) cells (9, 10). The enzyme and cellular results are shown in Table 1. These analogs are potent inhibitors (IC_{50} 7–63 nM) in both EGFR and ErbB-2 enzyme assays. In addition, the compounds are also active on ErbB-4, ranging in potency between 66 nM (compounds **6** and **8**) and 412 nM (compound **7**). Consistent with their enzyme activity, the [3,2-d]thienopyrimidines all had IC_{50}s of at least 500 nM or less in antiproliferative activity against HN5 and BT474 cell lines. The most potent analog in this series the 2-pyrrolidinyl derivative **8**, showed similar activity to lapatinib in these cell lines.

In contrast to their series A counterparts, compounds from series B are less active at both the enzyme and cellular level. The pyrrolidine analog **12**, for example, is at least 10-fold less potent than **8** versus EGFR in the enzyme assay, 5-fold less potent at the cellular level (HN5 cells), and ≈4-fold less active in the ErbB-2 enzyme and cellular proliferation (BT474) assays. Other analogs in series B are also less active than their isomeric counterparts in series A, with the exception of the simple acetylene derivative **10**, which had similar potency to **6** in the ErbB-2 cellular assay.

X-Ray Crystallography: Analog 6 Bound to ErbB-4 Catalytic Domain. The x-ray crystal structure of erlotinib and lapatinib bound to EGFR have both been reported (11, 12). As described previously, the structure of lapatinib in EGFR revealed that the bulky benzyloxy aniline head group induced a significant conformational shift of the enzyme relative to erlotinib. To clarify the binding mode of the thienopyrimidine analogs described herein, we sought to obtain analogous x-ray structures with EGFR and ErbB-4 in this series.
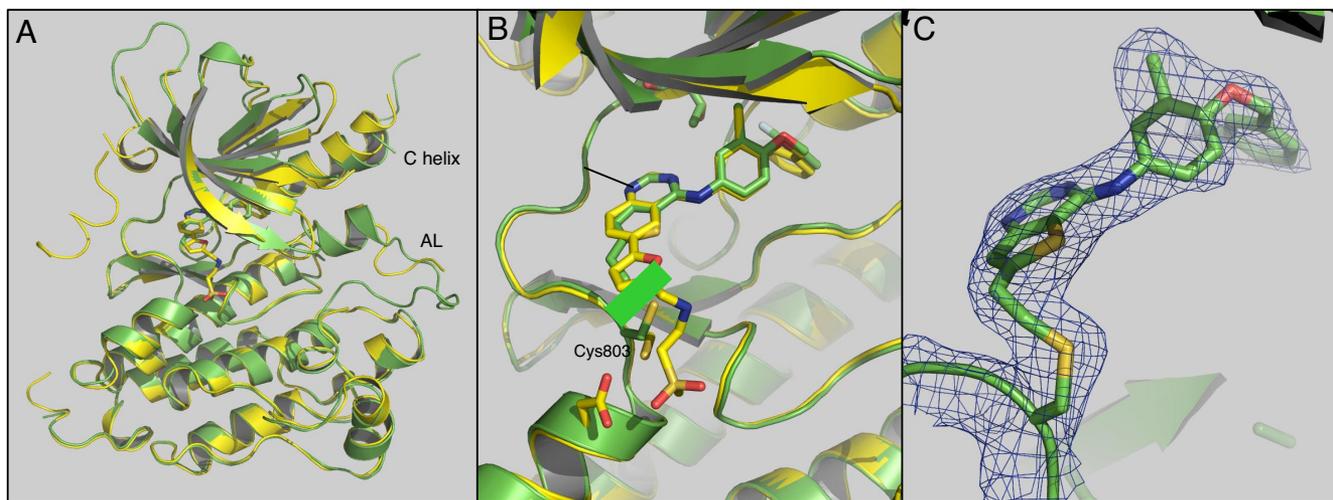
Fig. 3. X-ray crystal structure of thienopyrimidine 6 in ErbB-4. (A) Overlay of the ErbB-4 complexed with 6 (green) and EGFR complexed with lapatinib (yellow). (B) Overlay of the active sites of ErbB-4 (green) and EGFR (yellow). The covalent bond between ErbB-4 and 6 is shown as a dotted green line. The location of a hydrogen bond between the pyrimidine N1 of 6 and the hinge region of ErbB-4 is shown by a dashed line. (C) Omit map density for the ErbB-4 inhibitor complex contoured at 1 sigma.

Wood *et al.*

Table 1. Enzyme (40 min incubation) and cellular data (72 h incubation) for [3,2-d] (series A) and [2,3-d] (series B) thienopyrimidines

Compound	Series	R	Enzyme potency (IC$_{50}$), nM			Cellular potency (IC$_{50}$), nM		
			EGFR	ErbB-2	ErbB-4	HN5	BT474	HFF
6	A	H	24	12	66	657	396	4,029
7	A	(H$_2$N structure)	64	27	412	226	239	4,075
8	A	(pyrrolidine structure)	7	13	66	238	94	2,733
9	A	(aminopyrazine structure)	47	10	254	203	154	27,000
10	B	H	71*	19*	1,718*	1,826	696*	565
11[†]	B	(H$_2$N structure)	69*	44*	638*	710	643	21,500
12	B	(pyrrolidine structure)	109	54	2,301	536	205	2,700
13	B	(aminopyrazine structure)	372	52	1,349	262	161	24,500
3	—	—	11[‡]	9[‡]	367[‡]	120[‡]	100[‡]	12,000[‡]
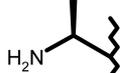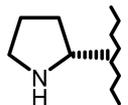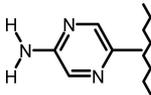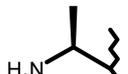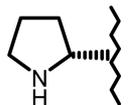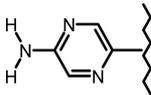
*$n = 1$ for this example, others $n >/= 2$. Variability of values in Table 2 were generally within 3-fold of one another.
[†]Formate salt.
[‡]Data for lapatinib are taken from ref. 10.

Although attempts to crystallize thienopyrimidine analogs such as **6** with EGFR were unsuccessful, inhibitor **6** complexed wi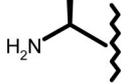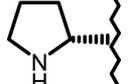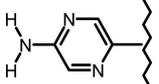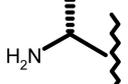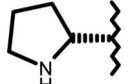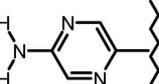th the catalytic domain of ErbB-4 produced crystals amenable to x-ray analysis. The crystal structure of analog **6** in ErbB-4 revealed several interesting features. The overall conformation of ErbB-4 is similar to that observed for EGFR complexed with lapatinib (Fig. 3*A*) (13). The protein is observed in an inactive conformation where the C helix is significantly shifted from its active position. The conformation of ErbB-4 bound to 6 is also similar to that of the conformation of an inactive V924R mutant EGFR reported by Zhang *et al.* (14) and stands in contrast to the active conformations of EGFR reported by Stamos, Zhang, and Yun (11, 13, 14). The pyrimidine N-1 atom of the inhibitor forms a hydrogen bond to the backbone NH of a methionine residue in the beta strand or hinge region. The inhibitor aniline substituent binds in the "backpocket" of the enzyme in a manner similar to that of lapatinib in EGFR (Fig. 3*B*) (12). Of key significance, the thienopyrimidine inhibitor ErbB-4 structure revealed a covalent bond between the Cys-803 sulfhydryl group and the acetylene terminus of the inhibitor (Fig. 3*C*) (15). This was clearly evident both from the distance between the sulfur atom and the carbon terminus (≈1.6 Å) and from the nonlinear orientation of the two carbon atoms of the C-6 substituent with the thienopyrimidine core. This covalent interaction suggested that alkylation of the conserved cysteine of the ErbB family active site might be a general property of this series.

Mass Spectrometry: Covalent Modification Assay. A facile protocol to quickly assess the ability of a small molecule to form a covalent adduct with EGFR was developed. In this method, an aqueous solution of the catalytic domain of EGFR was incubated at 20°C with an equimolar amount of inhibitor (1 μM each). After incubation of the two components, the sample was analyzed by LC/MS and the molecular mass was determined for the protein from the maximum entropy-transformed mass spectra. The contrasting behavior of the two ErbB inhibitors lapatinib and canertinib under these conditions was striking. Despite the slow-binding kinetic behavior of lapatinib with EGFR, the molecular mass of the enzyme after incubation with lapatinib was unchanged after 20 h incubation, consistent with reversible, noncovalent inhibition (12). In contrast, incubation of EGFR with **4** for 30 min led to the complete alkylation of protein as judged by the disappearance of EGFR protein (678–1020; molecular mass = 40,573 Da) and detection of an entity of molecular mass 485 Da higher (molecular mass = 41,058 Da) than parent protein. In the incubation of enzyme with compound **4**, modification of the enzyme was complete after 30 min, because no protein of unaltered molecular mass was recovered in this time frame. Interestingly, the acetylenic thienopyrimidines examined showed a wide range of alkylation reactivity in this assay (Table 2). At one end of the continuum, the pyrrolidine-containing compound **8** showed substantial but incomplete (83%) alkylation after 3 h and complete alkylation of EGFR after 20 h, as judged by the formation of a new entity with molecular mass 477 Da greater than native EGFR (678–1020). In contrast, the analog **9** whose structure lacks a basic, propargylic amine showed no covalent modification of EGFR after 20 h. Interestingly, even though both analogs contain cyclic amines (pyrrolidines) on the

Table 2. Alkylation of EGFR (%) by thienopyrimidine analogs

Compound	Series	R	Alkylation, of EGFR %	
			3 h	20 h
6	A	H	9	67
7	A	(H₂N-substituted acyclic amine)	0	15
8	A	(pyrrolidine)	83	100
9	A	(heteroaromatic piperazine)	0	0
11*	B	(H₂N-substituted acyclic amine)	0	19
12	B	(pyrrolidine)	4	24
13	B	(heteroaromatic piperazine)	0	0
4	–	–	100	100

*Tested as the trifluoroacetic acid salt; all others tested as free base form.

Table 3. *In vivo* activity of selected compounds in BT474 tumor xenografts

Compound	Series	Inhibition of BT474 tumor growth, %		
		10 mg/kg	30 mg/kg	100 mg/kg
3*	Quinazoline	19	38	86
7†	A	34	59	97
8†	A	38	86	109

*Dosed b.i.d. as HPMC/Tween suspension.
†Dosed b.i.d. as a solution in pH3 methanesulfonic acid.

were highly effective in this model, causing tumor regression at 100 mg/kg and strong inhibition of tumor growth at 30 mg/kg (Table 3).

Discussion

Our finding that alkynyl thienopyrimidine **6** forms a covalent adduct with an ErbB-4 construct at Cys-803 was a strikingly unexpected finding, because this compound does not contain a reactive Michael acceptor such as in canertinib. Nonetheless, our development of a facile and quantitative mass spectrometric method to assess the ability of small molecule kinase inhibitors to form covalent adducts with EGFR by using mass spectrometry demonstrates that alkylation of ErbB family enzymes is a general property of the series. Moreover, application of this method has enabled us to build an understanding of the structure–activity relationships of the covalent alkylation that are consistent with a unifying mechanistic hypothesis.

The data reported here reveal several striking trends: (*i*) although both series **A** and series **B** are active in enzyme and cellular assays against EGFR and ErbB-2, the [3,2-*d*] series **A** analogs generally possess greater ErbB family enzyme and cellular activity; (*ii*) members of the [3,2-*d*] series **A** also show greater covalent modification of EGFR than their corresponding counterparts from the [2,3-*d*] series **B**; (*iii*) analogs containing a basic propargylamine on the acetylene terminus tend to show greater covalent reactivity toward EGFR than analogs containing a nonbasic, heteroaromatic piperazine substituent (e.g., **9** and **13**). The terminal unsubstituted acetylenes **6** and **10** are less reactive than some other analogs in their respective series that have a basic propargylic amine substituent, although it is surprising that the [3,2-d] acetylenic thienopyrimidine **6** does show some reactivity, particularly at 20 h. Nano-LC/MS/MS sequencing experiments of enzymatically digested EGFR confirmed that modification of EGFR occurred on the active-site cysteine residue (797) that is conserved to Cys-803 in ErbB-4.ʲ Covalent structures of quinazoline alkylating agents to EGFR have been recently reported in which the enzyme has adopted an active-like orientation similar to that when bound to erlotinib (15).

These data suggest a mechanism for covalent modification of the Cys-797 of EGFR as shown in Fig. 4. We hypothesize that the pyrrolidine propargylamine **8** initially forms a noncovalent binding complex with the enzyme that enables it to form a hydrogen bond to the thiol proton of Cys-797 (see model in Fig. 4 *Inset*). Assisted by a neighboring aspartic acid residue (Asp-800), the basic amine then assists in deprotonation of the thiol, enabling nucleophilic

acetylene, ones containing acyclic amines (**7** and **11**) were only marginally reactive after 20 h. These data suggest that the pyrrolidine is a structural feature that assists in protein alkylation in the active site particularly well. Consistent with x-ray data that showed a covalent adduct with ErbB-4, thienopyrimidine **6** significantly (67%) modified EGFR after incubation for 20 h.

The rate of modification of EGFR by analog **8** and canertinib (**4**) was studied in greater detail [supporting information (SI) Fig. 5 and SI Table 4]. EGFR was incubated with compound under standard conditions and samples were injected for LC/MS analysis at various times. Enzyme modification by **8** was complete within 300 min. Fifty percent of the protein was modified in approximately 1 h. In contrast, 20% of EGFR was modified by 4 at the earliest possible injection time (≈1 min), and 100% was modified at the next time point (8 min).

The compound and enzyme concentrations used in this study are high relative to the estimated initial K_i for the compounds (<100 nM). We therefore assume that the time to binding equilibrium is minimal relative to the overall modification. With this assumption, we have modeled the covalent modification of EGFR by these compounds assuming a pseudo-first-order reaction rate 9 (see SI Fig. 6). The rate of the covalent step for analog **8** is estimated to be 0.01 per minute. In contrast, the rate of the covalent step for **4** is estimated to be > 0.1 per minute.

***In Vivo* Results.** To assess their potential antitumor activity, thienopyrimidines **7** and **8** were evaluated in a standard *in vivo* xenograft model by using the BT474 cell line (9, 12) Although somewhat less potent than lapatinib in cellular assays, both analogs showed very high *in vivo* activity. At doses of 30 and 100 mg/kg, both analogs

ʲDetermination of the covalent binding site on EGFR for compound **8**: covalently modified EGFR protein bands from a Coomassie-stained SDS/PAGE gel were excised (1-mm cubes), destained, reduced (4 mM DTT), and alkylated (4-vinylpyridine) according to a standard procedure. The gel pieces were then washed, crushed, dried, and digested with thermolysin (10 mM Tris, pH 8.0, 37°C, 18 h). After enzymatic digestion, nonpassively eluting peptides were further extracted from the crushed gel pieces by addition of 50% CH₃CN. Analysis of the thermolysin cleavage products by nano-ESI LC/MS/MS definitively confirmed Cys-797 as the site of covalent modification from the EGFR peptide observed at *m/z* 402.6 corresponding to H₂N-FGC-(**8**)-OH. Additional information concerning the identification of Cys-797 as the covalent binding site on EGFR is detailed in SI Fig. 5.
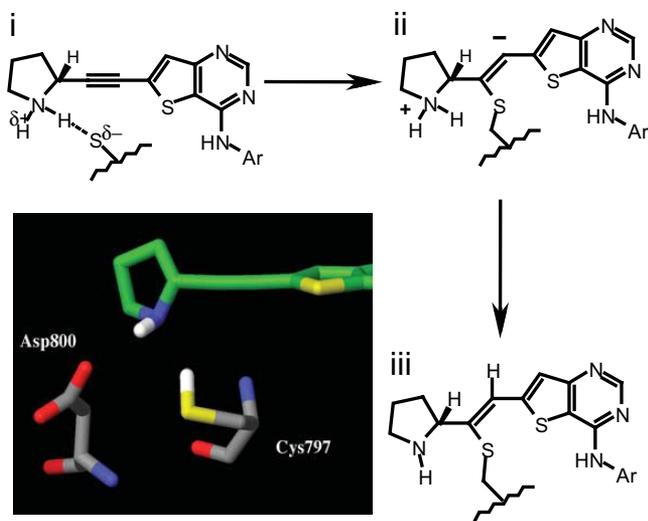
Wood *et al.*

Fig. 4. Proposed mechanism of covalent modification of pyrrolidine **8** with EGFR.

addition to the terminal acetylene carbon by the cysteine thiol anion. A related neighboring group effect facilitating addition of a nucleophile to an aromatic alkyne by hydroxyl has been observed (16). It should be pointed out that among the ≈12 kinases that contain a conserved cysteine in this position, only three non-ErbB family kinases that we are aware of have an Asp in the same relative position as that of EGFR, suggesting a possible mechanism of selectivity against those that do not.[k] This mechanism is consistent with the greater reactivity of the pyrrolidine analog **8** compared with other members of the [3,2-d] thienopyrimidine series that lack the basic amine. In addition, this mechanism also explains the finding that the [3,2-d] thienopyrimidines have higher reactivity than the [2,3-d] series, because the [3,2-d] thienopyrimidine core can afford greater resonance stabilization of the incipient anionic intermediate ii (Fig. 4) than can the isomeric thienopyrimidine core by placing a negative charge directly on a ring nitrogen on the pyrmidyl core.

The thienopyrimidines described herein are dual inhibitors of EGFR and ErbB-2 in both enzyme and cellular assays. Although the poor solubility of ErbB-2 enzyme preparations prevented us from developing an assay to test ErbB-2 alkylation, the presence of a homologous cysteine residue in ErbB-2 (Cys-797) makes it likely that these analogs can also alkylate this enzyme in an analogous manner. In fact, in an *in vivo* xenograft efficacy model with BT474 implants (which overexpress ErbB-2), both analogs **7** and **8** show excellent activity and are able to cause complete inhibition of tumor growth at doses at or >30 mg/kg b.i.d. (Table 3). As has been reported, lapatinib (**3**), a noncovalent inhibitor with a very slow off-rate, is also highly efficacious in this model, although perhaps not quite as efficacious on a per dose basis (Table 3) (12). In fact the single-dose oral exposure of analog **7** in mice in the corresponding formulations at the maximally

efficacious dose is substantially less than that of **3** ($AUC_{0\text{-inf}}$ 6.2 μg*h/ml at 113 mg/kg for **7** vs. 58.7 μg*h/ml at 100 mg/kg for **3**).[l] This suggests that the irreversible alkylation mechanism may compensate for the more limited exposure of **7**, producing potent *in vivo* activity.

The development of a straightforward mass spectroscopic method to assess the propensity of analogs in the [3,2-d] and [2,3-d] thienopyrimidine series to alkylate EGFR has revealed a striking range of reactivity among analogs tested. Although all of these compounds alkylate EGFR in this assay much less than canertinib at 3 h, some analogs fully modify EGFR over the course of 20 h. The range of reactivity shown across this series may represent a unique opportunity to design and deliver compounds whose balance between specific reactivity against ErbB family enzymes and that of off-target proteins may allow for the effective treatment of ErbB-2-driven tumors, with lowered risk of toxicity relative to more highly reactive ErbB family covalent modifying agents.[m] These findings have served as the basis for continued exploration in this area to design appropriately tuned compounds that will be reported in the future.

Materials and Methods

Synthesis of Analogs of 6-Ethynylthieno[3,2-d]- and 6-Ethynylthieno[2,3-d]pyrimidin-4-anilines. Either 6-bromo-4-chlorothieno[2,3-d]pyrimidine or 6-bromo-4-chlorothieno[3,2-d]pyrimidine was subjected to nucleophilic displacement of the chloride with 3-chloro-4-{[(3-fluorophenyl)methyl]oxy} aniline in refluxing isopropyl alcohol with catalytic concentrated HCl to give 6-bromo-N-(3-chloro-4-{[(3-fluorophenyl)methyl]oxy}phenyl)thieno[2,3-d] pyrimidin-4-amine or 6-bromo-N-(3-chloro-4-{[(3-fluorophenyl)methyl]oxy} phenyl)thieno[3,2-d]pyrimidin-4-amine, respectively. These substances were subjected to a Sonagashira coupling reaction with one equivalent of the appropriately substituted mono-substituted alkyne to give the 6-ethynylthieno[3,2-d]- and 6-ethynylthieno[2,3-d]pyrimidin-4-anilines.[n] The requisite mono-substituted alkynes and thienopyrimidine starting materials were prepared according to methods described in refs. 5–7.

ErbB2 and EGFR Enzyme Inhibition Assays. Compounds were tested for EGFR, ErbB-2, and ErbB-4 tyrosine kinase inhibition in peptide substrate phosphorylation assays. The purification of the proteins, details of the scintillation proximity assay, and data analysis are described in ref. 8.

Cellular Growth Inhibition Assays. Human breast (BT474), head and neck (HN5) and human foreskin fibroblasts (HFF) were cultured in low-glucose DMEM and the ability of the compound to inhibit proliferation as measured by methylene blue was determined. At 24 h after cells were plated, cells were exposed to

---

[k]Among the handful of kinases with a conserved Cys in the "lip" region of the kinase active site, those that also have an Asp in the same position as ErbB-2 and EGFR include JAK3, ITK, and BLK. Compound **8** was found to be inactive ($IC_{50} > 10$ μM) against ITK, whereas no data are available for JAK3 or BLK. In ErbB-4 this residue is glutamate, and because it is also acidic and in a sterically similar orientation, it should function similarly in the proposed mechanism. It should be noted that compound **8** has been shown to have >10-fold selectivity against 31/31 non-ErB family kinases in which it has been tested, and >100-fold selectivity against 30/31 such kinases. The limited number of kinases containing this CysXXAsp sequence is expected to also promote kinase selectivity for HKI-272, which contains a basic amine adjacent to a Michael acceptor.

[l]The drug exposures in the efficacy studies described in Table 3 with **3** and **8** were not determined. Nevertheless, the dramatic difference in AUCs in a separate but similar PK experiment strongly suggest that exposure of **3** in the efficacy study itself was significantly higher than that of **8**, as suggested in the text. In the PK experiment, female CD-1 mice were given a single oral dose of **7** in pH 3 methanesulfonic acid at 113 mg/kg or a single oral dose of **3** as HPMC/Tween suspension at 100 mg/kg versus b.i.d. dosing for 14 days in the efficacy study. Moreover, in another PK experiment, the exposure of **3** at 10 mg/kg in HPMC/0.1% HCl was also found to be much higher than **8** dosed in aqueous methanesulfonic acid at pH3 (1.6 vs. 0.67 h*μg/ml).

[m]Studies to assess the relative reactivity of agents described herein have demonstrated high selectivity for compounds in the thienopyrimidine series to Cys-797 of EGFR vs. thiols such as glutathionen (unpublished data).

[n]Representative Sonagashira coupling reaction procedure (compound **13**): A mixture of 6-bromo-N-(3-chloro-4-{[(3-fluorophenyl)methyl]oxy}phenyl)thieno[2,3-d]pyrimidin-4-amine hydrochloride (3.31 g, 6.6 mmol) (preparation described in WO 2003053446), Cu(I) I (44 mg, 0.23 mmol), 5-ethynyl-2-pyrazinamine (825 mg, 6.93 mmol, WO 2003053446), and bis (triphenylphosphine)dichloropalladium (II) (324.3 mg, 0.46 mmol) under a nitrogen atmosphere was covered with anhydrous tetrahydrofuran (68 ml) and triethylamine (3.3 ml, 23.8 mmol). The mixture was heated under a nitrogen atmosphere at 40°C for 1.5 h, allowed to cool to room temperature and partitioned between saturated aqueous NaHCO₃ and 5:1 CHCl₃/i-PrOH. The organic layer was dried over Na₂SO₄, filtered, and concentrated. Purification of the residue by silica gel chromatography eluting with a hexane/ethyl acetate gradient supplied product **13** (340 mg) along with recovered starting bromide (2.16 g). ^{1}H NMR (400 MHz, DMSO-d_6) δ 5.25 (s, 2H), 7.17–7.21 (m, 1H), 7.27–7.34 (m, 3H), 7.45–7.50 (m, 1H), 7.67 (dd, 1H, J = 9.0, 2.4 Hz), 7.87 (s, 1H), 8.03 (d, 1H, J = 2.2 Hz), 8.09 (s, 1H), 8.23 (s, 1H), 8.54 (s, 1H), 9.73 (s, 1H). HRMS (M+H)+ 503.0869, Calcd 503.0857.

compounds at varying concentrations and after 3 days relative cell number was estimated by using methylene blue staining. Details can be found in refs. 9 and 10.

Purification of EGFR 678-1020. A truncated form of the EGFR intracellular domain (amino acids 678-1020) was used for covalent modification studies because it gave high-quality data in mass spectrometry analysis. The protein was expressed in SF9 insect cells with a 6-His N-terminal tag by using baculovirus. The following buffers were used for purification: Buffer A, 50 mM Hepes pH 7.5, 500 mM NaCl, 20 mM imidazole; buffer B, 50 mM Hepes pH 7.5, 200 mM NaCl, 500 mM imidazole; buffer C, 20 mM NaPO$_4$, 100 mM NaCl pH 7.5; buffer D, 200 mM NaPO$_4$ pH 7.5; buffer E: 50 mM Hepes pH 7.5, 100 mM NaCl, 0.1 mM EDTA. In a 2.5-liter buffer A, 500 g of cell paste were lysed. The lysate was clarified by centrifugation in an SLA 1500 rotor at 12,000 rpm for 30 min, followed by filtration through a 0.2 μ PALL filter. The clarified lysate was applied to a Ni-Sepharose fast-flow column (5 × 4 cm) that had been previously equilibrated with Buffer A. The column was washed with 200 ml of buffer A and eluted with a 600 ml of gradient from 5 to 100% buffer B. Fractions were analyzed for the presence of EGFR protein by SDS/PAGE. EGFR-containing fractions were pooled and dialyzed against 16 liters of PBS (fraction 1, 320 ml). Fraction 1 was loaded onto a 2.5 × 4 cm 20 μ type I hydroxyapatite column previously equilibrated with buffer C. The column was washed with 50 ml of buffer C and eluted with 120 ml of linear gradient to 100% buffer D. Fractions containing EGFR were determined by SDS/PAGE and pooled (fraction 2, 30 ml). Fraction 2 was concentrated to 6 ml and applied to 2.5 x 300 cm Superdex S-75 gel-filtration column equilibrated with buffer E. The column was developed at 3 ml/min and fractions containing EGFR were pooled (fraction 3, 24 ml). NaCl was added to fraction 3 to a final concentration of 500 mM and CHAPS to 1 mM. This purification generated EGFR 678-1020 that was 95% pure as estimated by SDS/PAGE with a yield of 37 mg/g of cell paste.

Purification of ErbB4 690–999. Residues 690–999 of ErbB4 were fused to a 6× His tag (MKKGHHHHHHG) and ligated into a pFastBac1 vector (Invitrogen). The construct was transfected into *Spodoptera frugiperda* (*sf-9*) cells, single plaques were isolated, and high-titer stocks were generated. The protein was expressed and purified as described below. All operations were carried out at 4°C. Insect cells were resuspended and thawed in buffer A (25 mM Hepes pH 7.5, 750 mM NaCl, 10% glycerol, 25 mM imidazole) supplemented with a protease inhibitor mixture (Sigma), 1 mM MgCl$_2$, and 5 μg/ml of DNase I and RNase. The cells were lysed with a Polytron homogenizer (Brinkmann) and then centrifuged for 1 h at 30,000 × *g* (14,000 rpm) in a Sorvall SLA 1500 rotor. The pelleted material was discarded, and the supernatant was filtered through a 4.5 μ filter (PALL Corp.). The lysate was directly loaded onto a Ni-Chelating Sepharose FF column (Amersham Pharmacia). Before sample loading, the column was equilibrated with 5 column volumes (CVs) of buffer A. After sample loading, the column was washed for 5 CVs with buffer A. The protein was eluted with a 20 CVs linear gradient from 50 to 500 mM imidazole in buffer A. Fractions containing ErbB4K protein were analyzed by polyacrylamide gel electrophoresis and pooled. The pool was diluted 8-fold in buffer B (20 mM Hepes, 20 mM NaH$_2$PO$_4$, pH 6.8, 10% glycerol) and loaded onto Ceramic HA (Bio-Rad) column previously equilibrated in buffer B. Active ErbB4 flows through and does not bind. The flow-through fraction was brought to 0.6 M (NH$_4$)$_2$SO$_4$ by addition of a 2.5 M (NH$_4$)$_2$SO$_4$ stock solution and the sample applied to a Phenyl HIC column previously equilibrated in buffer E [20 mM Tris·HCl, pH 7.5, 0.6M (NH$_4$)$_2$SO$_4$]. A reverse linear gradient to 100% buffer F (20 mM

Tris·HCl, pH 7.5, 10% glycerol) was used to elute protein. Fractions containing pure ErbB4 were pooled, aliquoted, and stored at −80°C.

Assay for Quantification of EGFR Covalent Modification. Compounds were added with EGFR 678-1020 at a concentration of 1 μM each in 200 μl, 50 mM Mops, pH 7.5. The mixture was incubated for the indicated period at ambient temperature. The samples were then flash-frozen or immediately processed to determine the molecular mass by LC/MS (17). The sample volume that was injected was typically 10 μl. In each experiment, EGFR without any added compound was included as a control. The electrospray mass-to-charge spectra were transformed to the mass domain by using MaxEnt1 to obtain the maximum entropy mass spectra. Modified EGFR was identified by the appearance of a protein with an altered molecular mass compared with EGFR without added compound. In cases where EGFR was only partially modified, the fraction of the modified protein was estimated from the relative peak heights of each individual species. In all cases, the addition of only one ligand molecule was observed. Representative LC/MS traces are shown in SI Fig. 7.

ErbB-4 X-Ray Crystallography Study. Crystals of ErbB4 were obtained by the hanging drop vapor diffusion method. Protein ($\approx$4 mg/ml in 20 mM Hepes pH 7.5, 300 mM NaCl, 5 mM DTT, 1 mM CHAPS) was complexed with a 5-fold molar excess of inhibitor for 1 h before crystallization experiments. The protein–ligand complex was then mixed with an equal volume of reservoir (50 mM cacodylate pH 6.5, 100 mM ammonium acetate, 10 mM Mg acetate, 30% PEG8000) and incubated at 22°C. Crystals belonged to the tetragonal space group P4$_3$ with two molecules in the asymmetric unit and the following cell dimensions: a = 63.95, b = 63.95, c = 163.39, α = 90, β = 90, γ = 90.

Before data collection, glycerol and PEG400 were added to a final concentration of 25% and 5%, respectively, and the crystals were flash-frozen in liquid N$_2$. Data were collected at beamline 17-BM on a MAR-CCD detector in the facilities of the Industrial Macromolecular Crystallography Association Collaborative Access Team (IMCA-CAT) at the Advanced Photon Source, Argonne National Laboratory. The data were processed y by using HKL2000.

Structure Determination and Refinement. The structure of ErbB4 was solved by molecular replacement by using CNX and FGFR1 as a search model (molecule 1 of PDB ID code 1FGK). The search model contained FGFR1 residues 464–485, 491–500, 506–578, 592–647, and 651–761. Residues not conserved between FGFR1 and ErbB4 were truncated to alanine in the model. The correct solutions were the top two peaks in both the rotation and translation functions. Rigid body refinement gave an initial *R* factor of 48%. Multiple rounds of model building and refinement were carried out with QUANTA, CNX, and Refmac. The overall structure was confirmed by a composite omit map calculated with CNX. Analysis of the structure with PROCHECK indicated that all main-chain torsions fall within the allowed regions of the Ramachandran plot. Data statistics can be found in SI Table 4.

***In Vivo* Tumor Xenograft Inhibition Studies.** BT474 xenograft-implanted CB-17 SCID female mice were dosed b.i.d. for 14 days with vehicle (aqueous methanesulfonic acid, pH 3) or a solution of compound 7 or **8** in vehicle at 10, 30, or 100 mg/kg according to published methods (8–10).

1. Cockerill S, Lackey K (2002) *Curr Top Med Chem* 2:1001–1010.
2. Fry D, Bridges A, Denny W, Doherty A, Greis K, Hicks JL, Hook KE, Keller PR, Leopold WR, Loo JA, *et al.* (1998) *Proc Natl Acad Sci USA* 95:12022–12027.
3. Wissner A, Overbeek E, Reich M, Floyd M, Johnson B, Mamuya N, Rosford E, Discafani C, Davis R, Shi X, *et al.* (2003) *J Med Chem* 46:49–63.
4. Rabindran S, Discafani C, Rosfjord E, Baxter M, Floyd M, Golas J, Hallett W, Johnson B, Nilakantan R, Overbeek E, *et al.* (2004) *A Cancer Res* 64:3958.
5. Caferro T, Chamberlain S, Fan W-W, Rode H, Zhang C, Eck M, Weiss W, Shakat K (2003) WO Patent 2,003,053,446.
6. Badiang J, Dickerson S, Donaldson K, Harris P, Gaul M, Uehling D, Vanderwall D (2004) WO Patent 2,004,112,714.
7. Dickerson S, Emerson H, Hinkle K, Hornberger K, Sammond D, Smith S, Stevens K, Hubbard R, Petrov K, Reno M, Uehling D (2005) WO Patent 2,005,007,083.
8. Brignola P, Lackey K, Kadwell S, Hoffman C, Horne E, Carter H, Stuart J, Blackburn K, Moyer M, Allgood K, *et al.* (2002) *J Biol Chem* 277:1576–1585.

9. Rusnak D, Lackey K, Affleck K, Wood E, Alligood K, Rhodes N, Keith B, Murray D, Glennon K, Knight W, *et al.* (2001) *Mol Cancer Ther* 1:85–94.
10. Rusnak D, Affleck K, Cockerill S, Stubberfield C, Harris R, Page M, Smith K, Guntrip S, Carter M, Shaw R (2001) *Cancer Res* 61:7196–7203.
11. Stamos J, Sliwkoski M, Eigenbrot C (2002) *J Biol Chem* 277:46265–46272.
12. Wood E, Truesdale M, McDonald O, Yuan D, Hassell A, Dickerson S, Ellis B, Pennisi C, Horne E, Lackey K (2004) *Cancer Res* 64:6652–6659.
13. Zhang X, Gureasko J, Shen K, Cole P, Kuriyan J (2006) *Cell* 125:1137–1149.
14. Yun C-H, Boggon T, Li Y, Woo M, Greulich H, Meyerson M, Eck M (2007) *Cancer Cell* 11:217–227.
15. Blair J, Rauh D, Kung C, Yun, Fan W-W, Rode H, Zhang C, Eck M, Weiss W, Shakat K (2007) *Nat Chem Biol* 3:229–238.
16. Walters M, Cowen J, McWilliams J, Maligres P, Askin D (2000) *Tetrahedron Lett* 41:141–144.
17. White W, Wagner C, Hall J, Chaney E, Bindu G, Hofman K, Miller L, Williams J (2005) *Rapid Commun Mass Spectrom* 19:241–249.